

# Fast Neural Tangent Kernel Alignment, Norm and Effective Rank via Trace Estimation

James Hazelden<sup>\*†</sup>

**Abstract.** *The Neural Tangent Kernel (NTK) characterizes how a model’s state evolves over Gradient Descent. Computing the full NTK matrix is often infeasible, especially for recurrent architectures. Here, we introduce a matrix-free perspective, using trace estimation to rapidly analyze the empirical, finite-width NTK. This enables fast computation of the NTK’s trace, Frobenius norm, effective rank, and alignment. We provide numerical recipes based on the Hutch++ trace estimator with provably fast convergence guarantees. In addition, we show that, due to the structure of the NTK, one can compute the trace using only forward- or reverse-mode automatic differentiation, not requiring both modes. We show these so-called one-sided estimators can outperform Hutch++ in the low-sample regime, especially when the gap between the model state and parameter count is large. In total, our results demonstrate that matrix-free randomized approaches can yield speedups of many orders of magnitude, leading to faster analysis and applications of the NTK.*

**Key words.** neural tangent kernel, recurrent neural networks, automatic differentiation, knowledge distillation, rich and lazy learning, Hutchinson trace estimator, matrix-free methods

**1. Introduction.** The Neural Tangent Kernel (NTK) is a linear operator describing the evolution of a model’s state when parameters are tuned gradually with Gradient Descent (GD) [1]. The NTK can be analyzed with classical linear algebra metrics. For example, the NTK norm can be used as regularizer improving generalization [2, 3], alignment can quantify rich and lazy training regimes of GD [4, 5, 6, 7, 8] and effective rank can explain low-dimensional collapse of latent model dynamics during GD training [9, 10, 11]. All of these expressions can be expressed using the matrix trace [§3].

However, empirical NTK analysis at scale remains limited by computation and memory. Existing applications rely on constructing the finite-width NTK, requiring  $n^2$  evaluations, then taking a trace, or computing the trace through  $n$  matrix-vector products. Approaches to speeding up NTK construction have been proposed (e.g., [12]) as well as model pruning to compute approximate NTKs [13]. In the infinite-width limit, sketching and other randomized approaches have been applied [14]. However, in practice, analysis and applications of finite-width NTK are still confined to small datasets and simple architectures. In this work, we show randomized *matrix-free* estimators are a natural fit for efficiently working with finite-width NTKs. Specifically, we use the Hutch++ [15] to compute the NTK trace, norm, effective rank and alignment (Algorithm 1). Furthermore, we introduce a Hutchinson-style estimator for the NTK trace that relies only on reverse- or forward-mode Automatic Differentiation (AD), which can be faster than Hutch++ for small sample counts (Algorithm 2 and [§4]). This allows users to choose the AD mode based on package-specific constraints.

In total, we show speedups computing the trace and related quantities on the order of 10-100 times for an MLP [16] and 100-10,000 for a recurrent GRU [17], enabling NTK use in practical applications (Fig. 1). Our *primary contributions* are

1. **Matrix-free NTK trace estimation** with Hutch++ and a Hutchinson alternative that uses only reverse- or forward-mode AD probes [§3] [15, 18].
2. **Numerical validation** for an NTK tracking (1) the output of an MLP neural network [§4.1] and (2) the hidden state of a recurrent GRU [§4.2] [16, 17].
3. **Applications.** NTK norm, alignment, and effective rank [§3.3] and numerical validation of Hutch++ on each expression for an MLP trained on MNIST [§4.3].

<sup>\*</sup>Applied Mathematics, University of Washington & The Allen Institute, Seattle, WA.

<sup>†</sup>Correspondence: [jhazelde@uw.edu](mailto:jhazelde@uw.edu). Accompanying code: <https://github.com/meeree/kpflow/>.

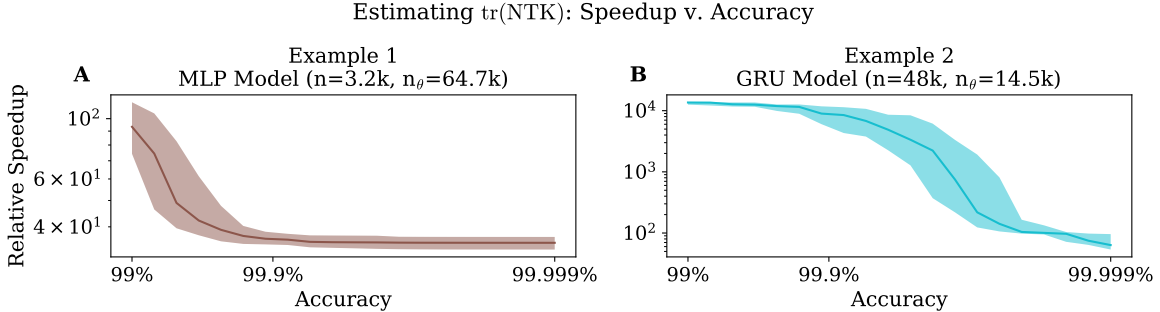


FIG. 1. **Approximating  $\text{tr}(\text{NTK})$ , speedup versus accuracy, summarizing the numerical results in [§4].** **A** corresponds to the MLP explored in [§4.1] with 3,200 NTK state-variables and around 64,700 parameters. Achieving 99% accuracy was about 80 times faster than exactly calculating the NTK trace explicitly with  $n$  evaluations, while achieving 99.999% accuracy was about 30 times faster. **B** corresponds to the GRU in [§4.2]. Reaching 99% accuracy was over 10,000 times faster, while 99.999% could be attained about 70 times faster. Here, each estimator from [§3] (Hutch++, RHutch, FHutch) was run 50 times, and we recorded which method reached each accuracy level the fastest, plotting the speedup versus the exact trace evaluation time. The curves show the median across runs and shaded regions show the 25<sup>th</sup> and 75<sup>th</sup> percentiles.

## 2. NTK Background.

**NTK Definition.** The empirical Neural Tangent Kernel (NTK) is a linear operator defining how a parameterized object evolves as the parameters update for a single Gradient Descent (GD) iteration. Consider a generic parameterized mapping from *parameters*,  $\theta \in P$ , to a *state*  $h \in H$ ,

$$(1) \quad h = h(\theta) \in H$$

Throughout, we assume  $\text{vec}(h) \in \mathbb{R}^n$ , the vectorized state, has  $n$  entries. Next, define the parameter Jacobian of this mapping  $J_\theta := \frac{dh}{d\theta}$ , which may be tensor-valued in general. Then, we can define two operations  $\text{vjp} : H \rightarrow P$ ,  $\text{jvp} : P \rightarrow H$  (vector-Jacobian and Jacobian-vector product, respectively). Specifically, given any *tangent* vector  $v \in H$  in the state space or parameters  $p \in P$  we define

$$(2) \quad \text{vjp}(v) := J_\theta^T v; \quad \text{jvp}(p) := J_\theta p$$

From this,  $\text{NTK} : H \rightarrow H$  is a linear operator defined by

$$(3) \quad \text{NTK}(v) := \text{jvp}(\text{vjp}(v)) = J_\theta J_\theta^T v \quad \text{for any } v \in H$$

Importantly,  $J_\theta$  is never explicitly constructed since this matrix can be prohibitively large. Performing  $\text{vjp}$  uses *reverse-Mode* Automatic Differentiation (AD), and  $\text{jvp}$  uses *forward-Mode* AD. We note that sometimes the left and right Jacobian above differ (the cross-NTK),  $J_\theta(x)J_\theta(x')$ , for different inputs  $x, x'$ . For simplicity, we assume the structure above, but Hutch++ (Algorithm 1) applies to this non-symmetric case immediately and the one-sided estimator (Algorithm 2) can be tweaked to apply, detailed in Proposition 1 in the Appendix [§6].

**Matvec Perspective.** In the above we defined the NTK by how it acts on inputs  $v \in H$ . Applying the NTK to a particular input  $v$  is typically referred to as a *matvec* [15]. Throughout this work, we only work with the *matvec* interface, never explicitly constructing the NTK. Constructing the NTK explicitly is infeasible for even small models. For example, if the  $h(\theta)$  represents the hidden state of an RNN over all evaluation times, then  $\text{vec}(h(\theta)) \in \mathbb{R}^{n_{\text{time}} \cdot n_{\text{batch}} \cdot n_{\text{hidden}}}$ . If  $n_{\text{time}} = n_{\text{batch}} = n_{\text{hidden}} = 100$ , a reasonably small model, then the NTK matrix has  $10^{12}$  entries. Sometimes the NTK can be compressed, e.g., by taking a trace over the hidden dimension [1], but it is clear that for larger models the cost incurred by constructing the full NTK is very prohibitive.

### 3. Methods.

**3.1. The Hutch++ Trace Estimator.** Throughout, we let  $G : H \rightarrow H$  denote a generic linear operator on the state-space  $H$ . A basic operation upon which much practical NTK metrics can be defined is the trace. In particular, for any basis  $Q = (q_i)_{i=1}^n$  of the space  $H$  we define

$$(4) \quad \text{tr}(G) := \sum_{i=1}^n q_i^T G q_i = \text{tr}(Q^T G Q)$$

This expression provides the simplest brute-force direct approach to computing the exact trace, performing  $n$  matvec evaluations with  $G$ . However, much prior work in the trace estimation literature has shown that far fewer matvecs can be used to randomly estimate  $\text{tr}(G)$  with high accuracy. A fast and simple approach for estimating this expression is Hutch++ [15]. Briefly, it relies on the observation that for effectively low-rank  $G$ , most of the terms  $q_i^T G q_i$  above will be almost zero. Hutch++ replaces the full matrix  $Q$  with a tall matrix of shape  $(n, m)$  for some sample count  $m$ , effectively only keeping the  $q_i$  that are not in the nullspace of  $G$  by a QR decomposition on a random sketch of  $G$ 's outputs. In addition, it estimates the trace contribution in the remaining space not spanned by the tall matrix  $Q$  (see [15] and [19] for a detailed introduction). Crucially, modern analyses have shown that Hutch++ estimates  $\text{tr}(G)$  for any  $G$  (not necessarily PSD) with variance  $O(1/m^2)$  as the sample count,  $m \rightarrow n$  [19]. Typically, very low sample counts can be used when, as we commonly observed for the NTK,  $G$  is effectively low rank (see Numerical Results [§4]). Below is a summary of the Hutch++ algorithm for estimating an NTK trace.

---

**Algorithm 1** Hutch++ NTK Trace Estimator

---

**Input:** Access to  $\text{NTK}(v)$  matvec for all  $v \in H$ . Number of samples  $m$

**Output:** Approximation to  $\text{tr}(\text{NTK})$

1: Draw $S, T \in \mathbb{R}^{n \times \frac{m}{3}}$ with i.i.d $\{+1, -1\}$ entries	$\text{// Or } \mathcal{N}(0, 1) \text{ entries}$
2: $Q \leftarrow \text{QR}(\text{NTK}(S))$	$\text{// Basis for range of NTK}$
3: $B \leftarrow (I - QQ^\top)T$	$\text{// Nullspace part of NTK range}$
4: <b>return</b> $\text{tr}(\text{NTK}(Q)^\top Q) + \frac{3}{m} \text{tr}(\text{NTK}(B)^T B)$	$\text{// Low rank + residual estimates}$

---

The choice  $\frac{m}{3}$  for the QR and `matvec` call is a hyperparameter that can be set, as long as the total `matvec` count is  $m$ . In practice, in Algorithms 1 and 2, we chose  $\lfloor \frac{m}{6} \rfloor$  for the QR probes, leaving  $m - \lfloor \frac{5m}{6} \rfloor$  `matvecs` for the remaining terms.

**3.2. One-Sided NTK Trace Estimators (RHutch / FHutch).** We find Hutch++ to be a robust and efficient estimator for very accurate traces. However, evaluating the NTK requires both `jvp` and `vjp` access (forward- and backward-mode AD). Sometimes one of these AD modes is not implemented or may bottleneck the trace estimation, as discussed below. To overcome this, we introduce two alternative Hutchinson-style estimators of the trace that rely on a single, specified AD direction (forward or backward) [18]. Specifically, since the NTK has the form  $JJ^\top$ , the trace can be estimated as

$$\text{tr}(JJ^\top) = \mathbb{E}_v [\|J^\top v\|_2^2] = \mathbb{E}_p [\|Jp\|_2^2],$$

where  $v \in H, p \in P$  are isotropic variables in the state- or parameter-space, respectively. Thus,  $\text{tr}(\text{NTK})$  can be estimated using only reverse-mode AD, ( $G(v) = \text{vjp}(v)$ , `RHutch`) or forward-mode AD, ( $G(p) = \text{jvp}(p)$ , `FHutch`). The algorithm below summarizes these estimators.

---

**Algorithm 2** One-Sided NTK Trace Estimators

---

**Input:** Either define  $G(v) = \text{vjp}(v)$  for any  $v \in H$  and  $d = \dim(H)$ , or  $G(p) := \text{jvp}(p)$  for any  $p \in P$  and  $d = \dim(P)$ . Number of samples  $m$ .

**Output:** Approximation to  $\text{tr}(\text{NTK})$

- 1: Draw  $S, T \in \mathbb{R}^{d \times \frac{m}{2}}$  with i.i.d.  $\{+1, -1\}$  entries // Or  $\mathcal{N}(0, 1)$
- 2:  $Q \leftarrow \text{QR}(S)$  // Optional orthogonalization
- 3:  $B \leftarrow (I - QQ^\top)T$  // Probes in the orthogonal complement
- 4: **return**  $\|G(Q)\|_F^2 + \frac{2}{m}\|G(B)\|_F^2$  // Low rank + residual estimates

---

**Viability.** RHutch/FHutch sample different spaces and rely on a single AD mode. They can be beneficial when  $\dim P$  is much larger than  $\dim H$ , or vice-versa. Also, for some architectures, GPU accelerated implementations may only exist for one AD mode. The variance of both estimators scales as  $O(1/m)$  [18]. For high accuracy, we recommend Hutch++, but show RHutch/FHutch can be faster in the small  $m$  regime, based on the architecture (see [§4]). Technically, the estimator in Algorithm 2 is not standard Hutchinson, instead using Haar-orthogonal probes and a residual control-variate, similar to Hutch++ but without sketching the NTK [19]. We used this form, since in practice it typically outperformed plain Hutchinson in our numerical experiments.

	Pros	Cons
<b>Hutch++</b>	$O(1/m^2)$ variance guarantee and robust	May be bottlenecked by either forward- or backward-mode AD
<b>One-Sided Hutchinson</b>	Can choose either forward- or backward-AD	Worse $O(1/m)$ variance guarantee

---

**3.3. Terms Involving the Trace.** Here, we discuss three practical applications of the NTK trace: norm, alignment and effective rank. Since each expression can be written using trace, Hutch++ can be applied in each case for rapid estimation.

**Frobenius Norm.** The NTK Frobenius norm has been used as a regularizer during training for so-called *knowledge distillation* [2, 3]. It describes total energy of the NTK operator, given by,

$$(5) \quad \|\text{NTK}\|_F^2 = \text{tr}(\text{NTK} \cdot \text{NTK}^\top)$$

This can be efficiently estimated by Hutch++ applied to the operator  $\text{NTK} \cdot \text{NTK}^\top$ , requiring two `vjp` and `jvp` calls per-evaluation.

**Alignment Between NTKs.** After a model is trained on a task, how much the NTK changes can quantify rich and lazy GD training regimes [4, 5, 6, 7, 8]. This can be measured by how much spans overlap, specifically, given NTKs with the same underlying state-space,  $\text{NTK}_1, \text{NTK}_2 : H \rightarrow H$ , their alignment is

$$(6) \quad \cos(\text{NTK}_1, \text{NTK}_2) := \frac{\text{tr}(\text{NTK}_1^T \text{NTK}_2)}{\|\text{NTK}_1\|_F \|\text{NTK}_2\|_F} \in [0, 1]$$

**Effective Rank.** The NTK effective rank can quantify how constrained and potentially low-dimensional GD updates are [9, 10, 11]. This can be expressed through the *participation ratio* (PR),

$$(7) \quad r_{eff}(\text{NTK}) := \frac{\text{tr}(\text{NTK})^2}{\text{tr}(\text{NTK} \cdot \text{NTK}^\top)} = n \cdot \cos^2(\text{NTK}, \text{Id}_H) \in [0, n]$$

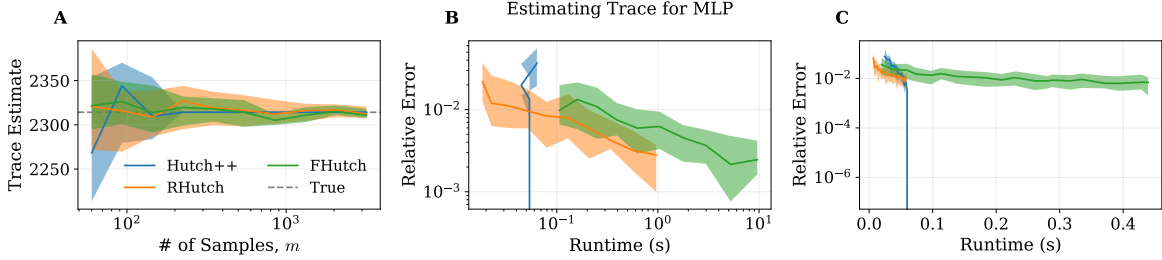


FIG. 2. **Estimating  $\text{tr}(\text{NTK})$  when  $h(\theta)$  tracks the output of an MLP neural network.** **A** illustrates the trace estimates for the three approaches in [§3]: Hutch++ (Algorithm 1) and the one-sided estimator (Algorithm 2) with forward- and backward-AD (FHutch and RHutch respectively). **B** shows the relative error  $\frac{|\text{tr}(\text{NTK}) - t_m|}{|t_m|}$  of each estimate,  $t_m$  versus runtime in seconds. For reference, exactly computing the trace took 1.96 seconds. **C** shows the low-runtime region of B in more detail with linearly scaled runtime, showing that FHutch is the slowest for this setup. Note Hutch++ obtained relative error below  $10^{-6}$  in about 0.06 seconds (about 33 times faster than the exact trace).

**3.3.1. One-Sided Variants.** For consistency and enabling future directions, in Appendix [§6] we prove a Proposition that facilitates estimation of NTK products of the form  $J_1 J_2^T J_3 J_4^T$  relying solely on either forward-mode or reverse-mode AD. We show that this enables one-sided estimation of the NTK norm, alignment, effective rank and cross-trace in the style of Algorithm 2. However, for now we find Hutch++ is simpler and generally outperforms these one-sided product estimators, so our numerical experiments for these expressions relied solely on Hutch++ [§3.3]. Variance reduction for these one-sided product estimators is a future direction (discussed in [§5]).

#### 4. Numerical Validation.

##### 4.1. NTK for the Output of a Deep MLP.

**Setup.** First, we consider the classical NTK setup of a deep Multi-Layer Perceptron (MLP) neural network [1]. We fix the hidden unit count at each layer as 64, use 15 total layers. As input to the network, we feed 50 distinct Gaussian 100-dimensional inputs into the first layer of the MLP,  $x \sim \mathcal{N}(0, 1)^{100}$ . This simple setup is chosen primarily to measure the validity of the trace estimators as runtime versus error, compared to the direct approach of computing the exact NTK trace with  $n$  matvecs. In this MLP case, the state  $h(\theta)$  reflects all activations of the output layer of the network, hence  $n = 3,200 = 50 \cdot 64$ . See Appendix [§6] for additional details. The parameter count,  $\dim P$ , is 64,704 in this case.

**Results.** Fig. 2 summarizes our results for this architecture. RHutch and FHutch denote the one-sided trace estimator in Algorithm 2 using  $G = \text{vjp}$  and  $G = \text{jvp}$ , respectively. Evaluating the full trace with 3,200 matvecs required around 1.96 seconds. By contrast, the Hutch++ estimator achieved relative error below  $10^{-6}$  in about 0.06 seconds, 50 times faster, using about 600 matvecs. Interestingly, for small sample counts,  $m < 100$ , the RHutch estimator using reverse-mode AD achieved the best accuracy in the fastest time. In this typical deep-learning setup, the parameter count is much higher than the state count. So, in this case RHutch samples a smaller space ( $H$ ) than  $\text{jvp}$  ( $P$ ). In many applications of the NTK, estimates of the trace with relative error  $10^{-2}$  (99% accurate) are acceptable, so using the one-sided estimator could provide a fast way to compute the NTK trace in this circumstance. However, if high accuracy is desired, the Hutch++ estimator always performs best. Finally, note in this case that the forward-mode estimator was slowest because it samples in the full parameter space,  $P$ , not the MLP output space  $H$ .

**Summary.** To summarize, if high accuracy is required, Hutch++ is fastest. RHutch can be faster in the low-accuracy regime provided  $\dim(H) < \dim(P)$ . By contrast, FHutch can be faster in

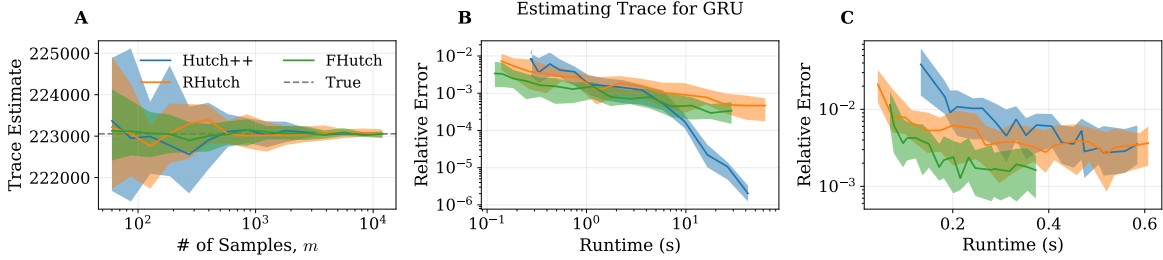


FIG. 3. **Estimating  $\text{tr}(\text{NTK})$  when  $h(\theta)$  tracks the hidden unit activations of a GRU neural network at every evaluation time.** Consistent with Fig. 2, A illustrates the trace estimates for Hutch++ and the one-sided Hutch estimator (Algorithms 1 and 2). B illustrates relative error  $\frac{|\text{tr}(\text{NTK}) - t_m|}{|t_m|}$  of each estimate,  $t_m$  versus runtime in seconds. In this case, exactly computing the trace with  $n$  matvecs took 1557.72 seconds (around 26 minutes). C shows the low-runtime region of B in more detail with linearly scaled runtime. In contrast to Fig. 2, FHutch performed fastest and both one-sided estimators outperformed Hutch++ for error above  $2 \cdot 10^{-3}$ . Hutch++ was fastest for accuracy above 99.9%.

this regime when  $\dim(P) < \dim(H)$ . The next experiment illustrates the latter case.

#### 4.2. NTK for the Hidden State of a Recurrent GRU.

**Motivation.** The NTK for recurrent models has been used to classify rich and lazy training regimes of recurrent models [4], characterize GD learning for linear RNNs [20] and explain low-dimensional collapse of latent dynamics [10]. However, forming the explicit matrix suffers from the cubic state size,  $n = B \cdot T \cdot H$  over batches, time and hidden or output units. Fundamentally, faster methods for probing the empirical NTK in the recurrent case are needed.

**Setup.** We let  $h(\theta)$  track the hidden state of a GRU recurrent network [17]. Similar to the MLP, we chose 64 hidden units, evaluated for  $T = 15$  timesteps on each input. Also, we provided the network with 50 random normal 10-dimensional inputs at every timestep. Unlike the output of the MLP, tracking the hidden state here means  $h(\theta)$  is a 3-tensor in  $\mathbb{R}^{64 \times 15 \times 50}$ , over all timesteps, not just the final layer, so it has with 48,000 entries. By contrast, since the GRU re-uses the weights for each layer, the parameter count is 14,592. Hence, in this case  $\dim(P) < \dim(H)$ .

**Results.** The results are summarized in Fig. 3. For reference, the full trace computation was very slow, taking about 26 minutes, or 1557.72 seconds. By contrast, 99% accuracy could be obtained in less than 0.1 seconds with FHutch. An accuracy of 99.99% (relative error  $10^{-4}$ ) took about 10 seconds with the Hutch++ estimator. Consistent with the prior findings, Hutch++ was fastest for high accuracy estimates, but the one-sided estimators could compete for low accuracy estimates. In contrast to the MLP output, however, here FHutch (using jvp) was faster than Hutch++ for errors above around  $10^{-3}$ . This is consistent with our prior summary, since the number of entries in  $h(\theta)$  exceeds the parameter count in this case and RHutch, FHutch sample from the state and parameter spaces, respectively.

#### 4.3. NTK Norm, Effective Rank and Alignment for MLP Trained on MNIST.

**Setup.** As a final application of the methods developed, we applied the Hutch++ estimator (Algorithm 1) to estimate the three trace-related quantities in Section 3.3: Frobenius norm, alignment and effective rank. Specifically, we trained an MLP model on MNIST with a single hidden layer of 256 neurons and 10 output units, yielding about 97% test-set accuracy. We then evaluated the norm and effective rank of the NTK after training,  $\text{NTK}_f$ , and alignment between the NTK before and after training ( $\cos(\text{NTK}_0, \text{NTK}_f)$ ). We used a testing set of 512 MNIST examples, yielding  $n = 5,120$ .

**Results.** We evaluated the three expressions with Hutch++ with results summarized in Fig. 4, sweeping the sample count  $m$ . There, we compare the estimation error to the relative runtime percentage

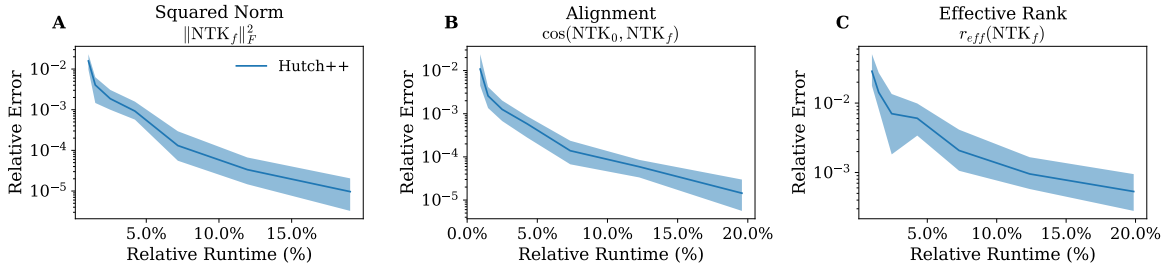


FIG. 4. **Relative runtime versus error for an MLP trained on MNIST, estimating the Frobenius norm, kernel alignment and the effective rank, respectively.** Here,  $NTK_f$  denotes the NTK of the model post-training while  $NTK_0$  is the NTK pre-training. **A-C** Plot the relative error versus the exact value, computed with exact trace evaluation. We plot these versus the percentage of total runtime required to compute the exact expression in each case (range 0% to 100%). Curves correspond to the median over 50 re-evaluations with Hutch++ and the shaded regions illustrate the 25<sup>th</sup> and 75<sup>th</sup> percentiles.

(in the range 0-100), taken as the ratio of the median runtime over 50 re-runs of the estimator, divided by the time for evaluating the exact expression. In all three cases, we found Hutch++ attained 99% accuracy (relative error  $10^{-2}$ ) with  $m = 60$  samples and in about 1% of the total runtime for the exact trace calculation, i.e., a 100 times speedup. An accuracy of  $10^{-4}$ , i.e., 99.99% accuracy, was attained 7.5% of the total runtime for the norm and alignment and around 25% of the runtime for the effective rank. In total, we found that Hutch++ can attain high accuracies for all three expressions in much shorter runtime. Note for larger models the expected speedups are larger since the Hutch++ estimator variance  $O(1/m^2)$  does not directly depend on  $n$ , instead the effective low-rank structure of the NTK.

**5. Discussion.** Our goal is to show that trace estimation is an effective tool for extracting statistics of the empirical NTK. With it, quantities such as the Frobenius norm, alignment, and effective rank can be computed efficiently. We primarily use Hutch++, a sketch-based trace estimator for generic linear operators with variance decaying as  $O(1/m^2)$  in the sample count  $m$ . We also show that a single AD mode pass (either `jvp` or `vjp`) suffices to compute the trace, which may be useful when only one direction is supported or fast. In the Appendix, we extend this to products of NTKs, yielding one-sided estimators for the norm and related quantities. Overall, trace estimation yields large speedups, potentially enabling the use of NTK metrics during training or for analysis of diverse architectures.

**Limitations and Future Directions.** Our one-sided Hutchinson variant is competitive with Hutch++ at coarse tolerances (e.g.,  $\sim 1\%$  relative error), but Hutch++ becomes faster and more accurate as  $m$  grows. Narrowing this gap requires injecting information about the NTK’s low-rank column space into the one-sided estimator. Specifically, Hutch++ effectively builds a QR basis from a sketch of NTK outputs, but one-sided methods see only `jvp` or `vjp`, not both, so they cannot form outputs directly. Thus, designing output-informed, one-sided estimators for the trace of the NTK or products of NTKs (as in Proposition 1) in the spirit of Hutch++ is a future direction.

Another future avenue is partial trace estimation. Recent work [21] extended Hutch++ to partial traces, reducing the NTK to a smaller matrix rather than a scalar. For example, if the state  $h \in \mathbb{R}^{n_{\text{batch}} \times n_{\text{out}}}$ , the partial trace over batches yields an  $n_{\text{out}} \times n_{\text{out}}$  matrix whose entries are block-wise traces of the NTK. Such partial averages provide a reduced, interpretable view of the NTK. They already occur in practice, e.g., it is common to average the NTK over hidden units [22]. For recurrent models, the NTK can be viewed as an operator on a 3-tensor domain and partial traces can be a powerful tool for analyzing such operators [10]. Thus, using partial trace estimators to rapidly form these reduced NTK views is another potential future direction.

**Code Availability.** Our NTK code is available at <https://github.com/meeree/kpflow/>. All experiments are reproduced in the file `experiments/trace_paper/main.py`.

## References.

- [1] Arthur Jacot, Franck Gabriel, and Clément Hongler. Neural tangent kernel: Convergence and generalization in neural networks. *Advances in Neural Information Processing Systems*, 31, 2018.
- [2] Jinlin Xiang, Minho Choi, Yubo Zhang, Zhihao Zhou, Arka Majumdar, and Eli Shlizerman. Neural tangent knowledge distillation for optical convolutional networks, 2025.
- [3] Arnav Sharma, Ahmed Wez, and Karthik Srikumar. On the relationship between neural tangent kernel frobenius distance and distillation sample complexity. In *Workshop on Lock-LLM at Neural Information Processing Systems (NeurIPS 2025)*, 2025. Poster.
- [4] Yuhan Helena Liu, Aristide Baratin, Jonathan Cornford, Stefan Mihalas, Eric Todd SheaBrown, and Guillaume Lajoie. How connectivity structure shapes rich and lazy learning in neural circuits. In *The Twelfth International Conference on Learning Representations*, 2024.
- [5] Haozhe Shan and Blake Bordelon. A theory of neural tangent kernel alignment and its influence on training, 2022.
- [6] Mario Geiger, Stefano Spigler, Arthur Jacot, and Matthieu Wyart. Disentangling feature and lazy learning in deep neural networks: an empirical study. *CoRR*, abs/1906.08034, 2019.
- [7] Alexander Atanasov, Blake Bordelon, and Cengiz Pehlevan. Neural networks as kernel learners: The silent alignment effect, 2021.
- [8] Tanishq Kumar, Blake Bordelon, Samuel J. Gershman, and Cengiz Pehlevan. Grokking as the transition from lazy to rich training dynamics, 2024.
- [9] Anonymous or list authors. Internal dynamics of neural networks through the ntk lens. *Preprint arXiv*, 2025.
- [10] James Hazelden, Laura Driscoll, Eli Shlizerman, and Eric Shea-Brown. Kpflow: An operator perspective on dynamic collapse under gradient descent training of recurrent networks, 2025.
- [11] Michael Murray, Hui Jin, Benjamin Bowman, and Guido Montúfar. Characterizing the spectrum of the ntk via a power series expansion. In *International Conference on Learning Representations (ICLR) 2023*, 2023. Poster.
- [12] Roman Novak, Jascha Sohl-Dickstein, and Samuel S Schoenholz. Fast finite width neural tangent kernel. In Kamalika Chaudhuri, Stefanie Jegelka, Le Song, Csaba Szepesvári, Gang Niu, and Sivan Sabato, editors, *Proceedings of the 39th International Conference on Machine Learning*, volume 162 of *Proceedings of Machine Learning Research*, pages 17018–17044. PMLR, 17–23 Jul 2022.
- [13] Yite Wang, Dawei Li, and Ruoyu Sun. Ntk-sap: Improving neural network pruning by aligning training dynamics, 2023.
- [14] Amir Zandieh, Insu Han, Haim Avron, Neta Shoham, Chaewon Kim, and Jinwoo Shin. Scaling neural tangent kernels via sketching and random features, 2021.
- [15] Raphael A. Meyer, Cameron Musco, Christopher Musco, and David P. Woodruff. Hutch++: Optimal stochastic trace estimation. *arXiv preprint arXiv:2010.09649*, 2020.
- [16] D. E. Rumelhart, G. E. Hinton, and R. J. Williams. Learning internal representations by error propagation. In *Parallel Distributed Processing: Explorations in the Microstructure of Cognition, Volume 1: Foundations*, pages 318–362. MIT Press, Cambridge, MA, 1986.
- [17] Kyunghyun Cho, Bart Van Merriënboer, Caglar Gulcehre, Dzmitry Bahdanau, Fethi Bougares, Holger Schwenk, and Yoshua Bengio. Learning phrase representations using rnn encoder–decoder for statistical machine translation. *arXiv preprint arXiv:1406.1078*, 2014.
- [18] M. F. Hutchinson. A stochastic estimator of the trace of the influence matrix for laplacian smoothing splines. *Communications in Statistics - Simulation and Computation*, 18(3):1059–1076, 1989.
- [19] Ethan N. Epperly, Joel A. Tropp, and Robert J. Webber. Xtrace: Making the most of every sample in stochastic trace estimation. *SIAM Journal on Matrix Analysis and Applications*, 45(1):1–23, 2024.

- [20] Blake Bordelon, Jordan Cotler, Cengiz Pehlevan, and Jacob A. Zavatone-Veth. Dynamically learning to integrate in recurrent neural networks, 2025.
- [21] Tyler Chen, Robert Chen, Kevin Li, Skai Nzeuton, Yilu Pan, and Yixin Wang. Faster randomized partial trace estimation. *SIAM Journal on Scientific Computing*, 46(6):A3427–A3447, November 2024.
- [22] Jiaming Xu and Hanjing Zhu. Overparametrized multi-layer neural networks: Uniform concentration of neural tangent kernel and convergence of stochastic gradient descent. *Journal of Machine Learning Research*, 25(1):1–83, 2024.
- [23] Adam Paszke, Sam Gross, Francisco Massa, Adam Lerer, James Bradbury, Gregory Chanan, Trevor Killeen, Zeming Lin, Natalia Gimelshein, Luca Antiga, Alban Desmaison, Andreas Köpf, Edward Yang, Zach DeVito, Martin Raison, Alykhan Tejani, Sasank Chilamkurthy, Benoit Steiner, Lu Fang, Junjie Bai, and Soumith Chintala. Pytorch: An imperative style, high-performance deep learning library, 2019.

## 6. Appendix.

**6.1. Implementation Details.** All numerical experiments were implemented in Pytorch [23]. GPU acceleration naturally applies to all the estimators, but here we ran all experiments on a CPU on a single desktop machine in this work. We implement the direct trace computation by forming  $\text{NTK}_{\text{eval}} = \text{NTK} \cdot I_H$  with  $n$  matvec calls against the standard unit coordinates  $e_i$  in  $H$ . To accelerate these batched products, we use torch `vmap` instead of looping over evaluations, both in the direct trace estimator and the approximate estimators. As a baseline to ground runtime comparisons, we verified that Hutch++ with  $m = n$  matvec evaluations typically produced a runtime around 80 – 120% of the direct estimator. Thus, setting the sample count  $m$  to the total dimension  $n$  produced a speed-up of around 1, indicating around the same amount of runtime. This ensured that runtime numbers are reliable and not inflated by specific implementation of the individual estimators.

**6.2. One-Sided NTK Product Estimator.** In the main text, we show in Algorithm 2 that the NTK trace can be approximated with a Hutchinson estimator using only one AD mode (reverse, `vjp`, or forward, `jvp`). Here, we show this extends to products of NTKs, yielding one-sided estimators for the norm, alignment, effective rank, as well as the case where  $\text{NTK} = J_1 J_2^T$  with distinct Jacobians on the left and right side (e.g., evaluated on the testing and training set, respectively). This result is summarized in the following Proposition.

**Proposition 1.** Let  $J_1, J_2, J_3, J_4 : P \rightarrow S$  be operators mapping the parameter space to the state space. Then, letting  $u, v \in H$  be independent random vectors such that  $\mathbb{E}[u] = \mathbb{E}[v] = 0$  and  $\mathbb{E}[uu^\top] = \mathbb{E}[vv^\top] = I$  (e.g., uniform  $\{+1, -1\}$  or  $\mathcal{N}(0, 1)$  entries). Then,

$$\text{tr}(J_1 J_2^\top J_4 J_3^\top) = \mathbb{E}[\langle J_1^\top u, J_2^\top v \rangle \cdot \langle J_4^\top u, J_3^\top v \rangle],$$

yielding a reverse-mode only estimator. Likewise, probing in the parameter space: if  $p, q \in P$  denote random vectors with  $\mathbb{E}[p] = \mathbb{E}[q] = 0$ ,  $\mathbb{E}[pp^\top] = \mathbb{E}[qq^\top] = I$ , then

$$\text{tr}(J_1 J_2^\top J_3 J_4^\top) = \mathbb{E}[\langle J_4 p, J_1 q \rangle \cdot \langle J_3 p, J_2 q \rangle],$$

yielding a forward-mode only estimator.

*Proof:*

Let  $A := J_1 J_2^T, B := J_3 J_4^T$ , so we want to estimate  $\text{tr}(AB)$ . By the standard Hutchinson estimator [18], assuming  $u, v \sim H$  denote random variables as in the proposition and expand

$$\begin{aligned} \mathbb{E}[\langle J_1^\top u, J_2^\top v \rangle \cdot \langle J_4^\top u, J_3^\top v \rangle] &= \mathbb{E}[\langle J_1^\top u, J_2^\top v \rangle \cdot \langle J_3^\top v, J_4^\top u \rangle] \\ &= \mathbb{E}[u^T J_1 J_2^\top v v^T J_3 J_4^\top u] \\ &= \mathbb{E}[u^T A v v^T B u] \end{aligned}$$

Marginalizing over  $u$ , we have

$$\mathbb{E}[u^T A v v^T B u | u] = u^T A \mathbb{E}[v v^T] B u,$$

using the assumptions thus yields

$$\mathbb{E}[u^T A v v^T J_4 J_3^\top u | u] = u^T A B u$$

So,

$$\mathbb{E}[u^T A v v^T B^T u] = \mathbb{E}[u^T A B^T u] = \text{tr}(AB).$$

This proves the reverse-mode estimator. For the forward mode, we have

$$(8) \quad \text{tr}(J_1 J_2^T J_3 J_4^T) = \text{tr}(J_4^T J_1 J_2^2 J_3)$$

and apply the same theorem to the matrices  $\hat{J}_1 = J_4^T, \hat{J}_2 = J_1^T, \hat{J}_3 = J_2^T, \hat{J}_4 = J_3^T$ , yielding

$$(9) \quad \text{tr}(J_1 J_2^T J_3 J_4^T) = \text{tr}(\hat{J}_1 \hat{J}_2^T \hat{J}_3 \hat{J}_4^T)$$

$$(10) \quad = \mathbb{E}[\langle \hat{J}_1^\top p, \hat{J}_2^\top q \rangle \cdot \langle \hat{J}_4^\top p, \hat{J}_3^\top q \rangle]$$

$$(11) \quad = \mathbb{E}[\langle J_4 p, J_1 q \rangle \cdot \langle J_3 p, J_2 q \rangle]$$

yielding the forward-mode estimator. Note implicitly here that the domains are different:  $p, q$  are samples from the parameter space  $P$  while  $u, v$  are samples from the  $H$  space  $\square$

From this, we can estimate the NTK norm,

$$(12) \quad \|\text{NTK}\|_F^2 = \text{tr}(\text{NTK} \cdot \text{NTK}^T)$$

$$(13) \quad = \mathbb{E}[\langle \text{vjp}(u), \text{vjp}(v) \rangle^2] = \mathbb{E}[\langle \text{jvp}(p), \text{jvp}(q) \rangle^2],$$

where the  $u, v$  form is the reverse-mode estimate and the  $p, q$  form is the forward-mode estimate.

Likewise, the alignment. Using the notation  $\text{NTK}_i(v) = \text{jvp}_i(\text{vjp}_i(v))$  for  $i = 1, 2$ , Proposition 1 yields the following expression

$$(14) \quad \cos(\text{NTK}_1, \text{NTK}_2) = \frac{\mathbb{E}[\langle \text{vjp}_1(u), \text{vjp}_1(v) \rangle \langle \text{vjp}_2(u), \text{vjp}_2(v) \rangle]}{\sqrt{\mathbb{E}[\langle \text{vjp}_1(u), \text{vjp}_1(v) \rangle^2] \mathbb{E}[\langle \text{vjp}_2(u), \text{vjp}_2(v) \rangle^2]}}$$

$$(15) \quad = \frac{\mathbb{E}[\langle \text{jvp}_2(p), \text{jvp}_1(q) \rangle^2]}{\sqrt{\mathbb{E}[\langle \text{jvp}_1(p), \text{jvp}_1(q) \rangle^2] \mathbb{E}[\langle \text{jvp}_2(p), \text{jvp}_2(q) \rangle^2]}}$$

Finally, the effective rank is given by

$$(16) \quad r_{eff}(\text{NTK}) = \frac{\mathbb{E}[\|\text{vjp}(u)\|_2^2]}{\mathbb{E}[\langle \text{vjp}(u), \text{vjp}(v) \rangle^2]} = \frac{\mathbb{E}[\|\text{jvp}(p)\|_2^2]}{\mathbb{E}[\langle \text{jvp}(p), \text{jvp}(q) \rangle^2]}$$

We found that the one-sided trace estimator could be faster than Hutch++ for trace predictions with low accuracy (around 99%). However, we find for now that the one-sided product estimators detailed here are typically slower than Hutch++ in all cases. Indeed, they rely on sampling independently  $u, v \sim H$  or  $p, q \sim P$  without any information about the NTK column space. Incorporating information about the NTK into these estimates, as in Hutch++, could be a future direction for improving the runtime of the one-sided estimators. We provide these here for future reference and directions.